



## OPEN ACCESS

## EDITED BY

Dafa Shi,  
Second Affiliated Hospital of Shantou  
University Medical College, China

## REVIEWED BY

Kuanjun He,  
Inner Mongolia University for Nationalities,  
China

Mike Zastrozhin,  
PGxAI Inc., United States

## \*CORRESPONDENCE

Wei Qin

✉ 179433035@qq.com

RECEIVED 30 April 2025

ACCEPTED 21 August 2025

PUBLISHED 04 September 2025

## CITATION

Lv J, Wang X and Qin W (2025)  
Integrated bioinformatics and machine  
learning identify S100A9 and VGLL1  
as hub genes for schizophrenia.  
*Front. Psychiatry* 16:1621219.  
doi: 10.3389/fpsyt.2025.1621219

## COPYRIGHT

© 2025 Lv, Wang and Qin. This is an open-access article distributed under the terms of the [Creative Commons Attribution License \(CC BY\)](https://creativecommons.org/licenses/by/4.0/). The use, distribution or reproduction in other forums is permitted, provided the original author(s) and the copyright owner(s) are credited and that the original publication in this journal is cited, in accordance with accepted academic practice. No use, distribution or reproduction is permitted which does not comply with these terms.

# Integrated bioinformatics and machine learning identify S100A9 and VGLL1 as hub genes for schizophrenia

Jiankang Lv<sup>1</sup>, Xueru Wang<sup>2</sup> and Wei Qin<sup>3\*</sup>

<sup>1</sup>Department of Severe Psychiatry, Shaoxing Seventh People's Hospital (Affiliated Mental Health Center, Medical College of Shaoxing University), Shaoxing, Zhejiang, China, <sup>2</sup>Department of Psychiatry, Shan Dong Daizhuang Hospital, Jining, Shandong, China, <sup>3</sup>Department of Psychiatry, Shandong Mental Health Center Affiliated to Shandong University, Jinan, Shandong, China

**Background:** Schizophrenia (SCZ) is a debilitating neuropsychiatric disorder with unclear etiology, involving complex interactions between genetic and environmental factors. Current diagnostic methods rely on subjective clinical assessments, and existing treatments often fail to address cognitive and negative symptoms adequately. Identifying key biomarkers for SCZ is crucial for improving diagnosis and developing targeted therapies.

**Methods:** This study integrated bioinformatics analysis and machine learning approaches to identify potential biomarkers for SCZ. Transcriptomic data from five independent cohorts were obtained from the GEO database. Differential expression analysis and Robust Rank Aggregation (RRA) were used to identify significant differentially expressed genes (DEGs). Protein-protein interaction (PPI) network, Least Absolute Shrinkage and Selection Operator (Lasso) regression and Random Forest (RF) were employed to screen for hub genes. The diagnostic model was constructed using logistic regression. The receiver operating characteristic (ROC) curve was used to evaluate diagnostic accuracy of the model, and nomograms and calibration curves were performed to evaluate their clinical applicability. Functional enrichment analyses and single-sample Gene Set Enrichment Analysis (ssGSEA) were conducted to explore the underlying mechanisms of the identified hub genes.

**Results:** S100A9 and VGLL1 were determined as potential diagnostic biomarkers for SCZ. The diagnostic model demonstrated robust diagnostic performance in the training cohorts (AUC = 0.806) and external validation cohorts (AUC = 0.702, 0.666 and 0.739). Functional enrichment analyses revealed that DEGs related to VGLL1 and S100A9 were primarily involved in immune system regulation and signaling pathways such as PI3K-Akt signaling pathway. ssGSEA showed significant increases in the infiltration levels of five immune cell types (CD56bright natural killer cells, MDSCs, mast cells, natural killer cells, and plasmacytoid dendritic cells) in SCZ patients, with strong positive correlations between S100A9 and these immune cell infiltrations.

**Conclusion:** Our study identified S100A9 and VGLL1 as potential biomarkers for SCZ, highlighting their roles in immune regulation. These findings provide new insights into the pathogenesis of SCZ and suggest potential diagnostic targets.

## KEYWORDS

schizophrenia, S100A9, VGLL1, bioinformatics analysis, machine learning

# 1 Introduction

Schizophrenia (SCZ) is a debilitating neuropsychiatric disorder affecting over 20 million individuals worldwide, characterized by a triad of positive symptoms (e.g., hallucinations), negative symptoms (e.g., social withdrawal), and cognitive dysfunction (1, 2). Despite its profound societal burden, the etiology of SCZ remains poorly understood. It is hypothesized that SCZ is associated with dysregulation of neurotransmission, defects in synaptic plasticity, and interactions between the nervous and immune systems (3). Current diagnosis relies on subjective clinical evaluations, while first-line antipsychotics (primarily targeting dopamine D2 receptors) exhibit variable efficacy and often fail to ameliorate cognitive or negative symptoms, accompanied by metabolic and extrapyramidal side effects (4). These limitations underscore the critical need for objective diagnostic tools and mechanism-based therapies.

The identification of biomarkers could bridge this gap by elucidating disease pathways and enabling targeted interventions. In oncology, biomarkers such as PD-L1 expression guide immunotherapy selection (5), while in neurodegenerative diseases, cerebrospinal fluid A $\beta$ 42/tau ratios aid Alzheimer’s diagnosis (6). In contrast, SCZ research faces a stark biomarker deficit. Although studies have proposed potential candidates (e.g., elevated IL-6 levels, hippocampal volume reduction, or polygenic risk scores) (7–9), none have achieved clinical validation due to heterogeneity across cohorts, low effect sizes, and poor reproducibility. This disparity highlights the urgency of discovering robust biomarkers specific to SCZ’s multifactorial pathology.

Emerging advances in machine learning provide powerful tools to decode complex biomarker patterns from high-dimensional omics data. Machine learning algorithms such as Least Absolute Shrinkage and Selection Operator (Lasso) regression and Random Forest (RF) have demonstrated success in other neuropsychiatric disorders (10). For example, Lasso-based models identified blood mRNA biomarkers predictive of major depressive disorder (11), while RF classifiers achieved >70% accuracy in distinguishing autism subtypes using metabolomic profiles (12). In addition, preliminary machine learning have linked gene co-expression networks to SCZ to stratify patient subgroups (13). This study aims to combine comprehensive bioinformatics analyses with machine learning to identify hub genes and molecular pathways

from transcriptomic datasets. Our findings seek to unravel potential mechanisms underlying SCZ pathogenesis and propose novel biomarker candidates for diagnosis and therapeutic development.

# 2 Materials and methods

## 2.1 Data acquisition and integration

This study retrieved five SCZ-related microarray datasets (GSE12654, GSE21935, GSE17612, GSE53987, GSE38481) from the Gene Expression Omnibus (GEO) database, comprising a total of 224 brain tissue samples (112 SCZ and 112 controls) and 37 whole blood sample (22 SCZ and 15 controls). Detailed dataset information is provided in Table 1. Quantile normalization was performed using the “limma” package to eliminate technical variability, and the ComBat algorithm was applied to correct inter-platform batch effects. After quality control, GSE12654 and GSE21935 were merged as the training cohort, while GSE17612, GSE53987 and GSE38481 served as independent external validation cohorts. The effectiveness of data integration was validated using boxplots and principal component analysis (PCA) generated by ggplot2.

## 2.2 Identification of differentially expressed genes

Differential expression analysis was conducted on the training cohort, GSE12654 and GSE21935 using the “limma” package, with screening criteria set at p-value <0.05 and |logFC| > 0.585 (14, 15). Heatmap and volcano plots of DEGs were generated using “pheatmap” and “ggplot2” packages, respectively.

## 2.3 Robust rank aggregation analysis

The RRA algorithm integrates gene ranking information across datasets via a probabilistic model to identify consistently significant DEGs across multiple independent datasets. In this study, RRA was applied to rank up- and down-regulated DEGs from all datasets based on logFC. Aggregated ranking scores were used to compute

TABLE 1 Detailed information of GEO datasets.

Datasets	Platforms	Sample source	Control	SCZ	Type
GSE12654	GPL8300	prefrontal cortex (BA10)	15	13	array
GSE21935	GPL570	temporal cortex (BA22)	19	23	array
GSE17612	GPL570	prefrontal cortex (BA10)	23	28	array
GSE53987	GPL570	Hippocampus Pre-frontal cortex (BA46) Associative striatum	55	48	array
GSE38481	GPL6883	Whole blood	22	15	array

p-value, and genes with p-value <0.05 and  $|\log FC| > 0.585$  were selected as DEGs. RRA analysis was implemented using the “RobustRankAggreg” package.

## 2.4 Enrichment analysis

Gene Ontology (GO) and Kyoto Encyclopedia of Genes and Genomes (KEGG) pathway enrichment analyses were performed using the “clusterProfiler” and “org.Hs.eg.db” packages. Significantly enriched GO terms and KEGG pathways were defined as those with p-value <0.05.

## 2.5 Protein-protein interaction network

PPI networks of DEGs were constructed using the STRING database and visualized with Cytoscape software. Feature DEGs were identified using 10 topological network algorithms (MCC, MNC, etc) via the cytoHubba plugin.

## 2.6 Machine learning

Lasso regression and RF were employed for hub genes selection. Lasso regression is a linear regression method used for feature selection and sparse modeling. It incorporates an L1 regularization term into the objective function to select fewer features, thereby reducing the risk of overfitting. In this study, Lasso regression was implemented using the “glmnet” package with the following parameters: family = binomial, type.measure = class, alpha = 1, and nfold = 10. RF, an ensemble learning method based on decision trees, was employed to capture non-linear relationships and assess feature importance. By constructing multiple decision trees and combining their predictions, RF enhances model accuracy and controls overfitting. The RF algorithm was performed using the “randomForest” package with ntree = 500. Feature importance was evaluated using the Gini coefficient, with a threshold of >2 used for selecting features DEGs.

## 2.7 Construction and validation of the diagnostic model

We utilized the “glm” function from the “glmnet” package to construct a logistic regression model. This function is a standard tool for fitting generalized linear models, particularly suitable for logistic regression analysis in binary classification problems. The expression level of feature DEGs was severed as the independent variable, with the disease diagnosis outcome (SCZ = 1, Control = 0) as the dependent variable. The parameter was set as family = binomial (link = ‘logit’). The formula of the model:  $y = \beta_0 + \beta_1 X_1 + \beta_2 X_2 + \beta_3 X_3 + \dots + \beta_i X_i$  ( $\beta$  was coefficient, X was the expression level of genes). Diagnostic performance was evaluated via receiver operating characteristic (ROC) curve in the training cohort and

external validation cohorts. The nomogram for predicting disease risk was constructed using the “rms” package, and the clinical applicability of the model was assessed through a calibration curve.

## 2.8 Immune infiltration analysis

single-sample gene set enrichment analysis (ssGSEA) quantified infiltration levels of 28 immune cell subtypes (16, 17). Wilcoxon rank-sum test was used to compare immune cell infiltration between SCZ patients and controls. Spearman’s rank correlation analyzed associations between hub genes and immune cells.

# 3 Results

## 3.1 Identification of DEGs

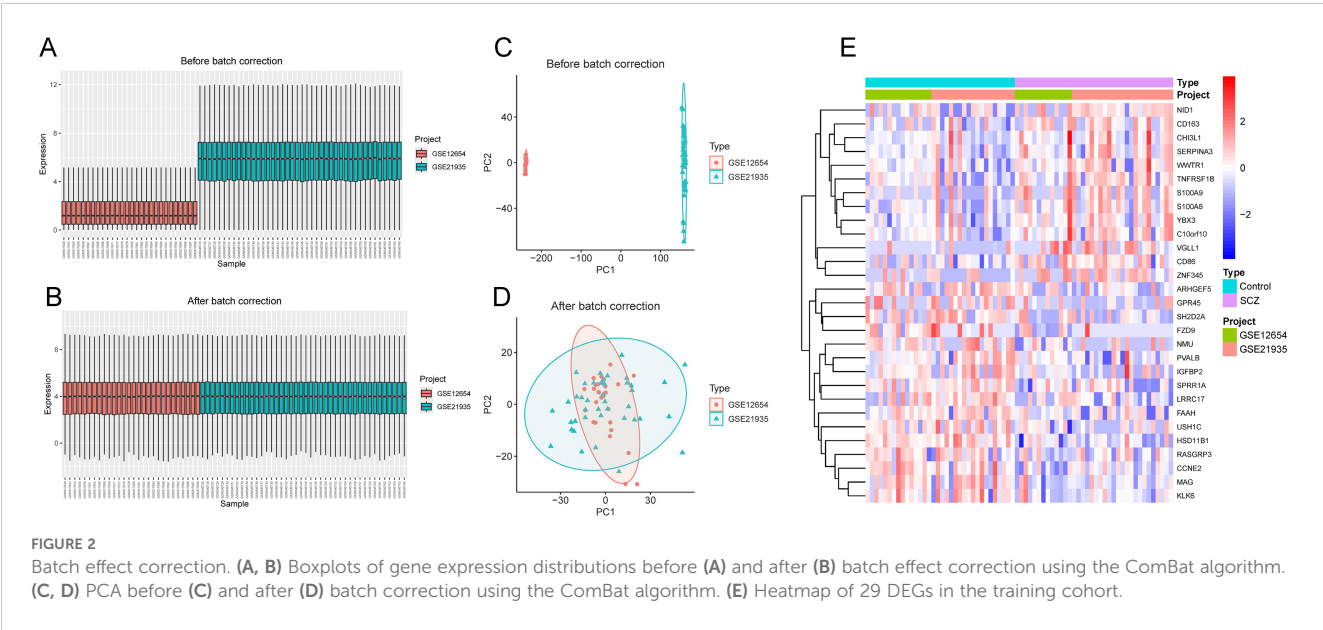
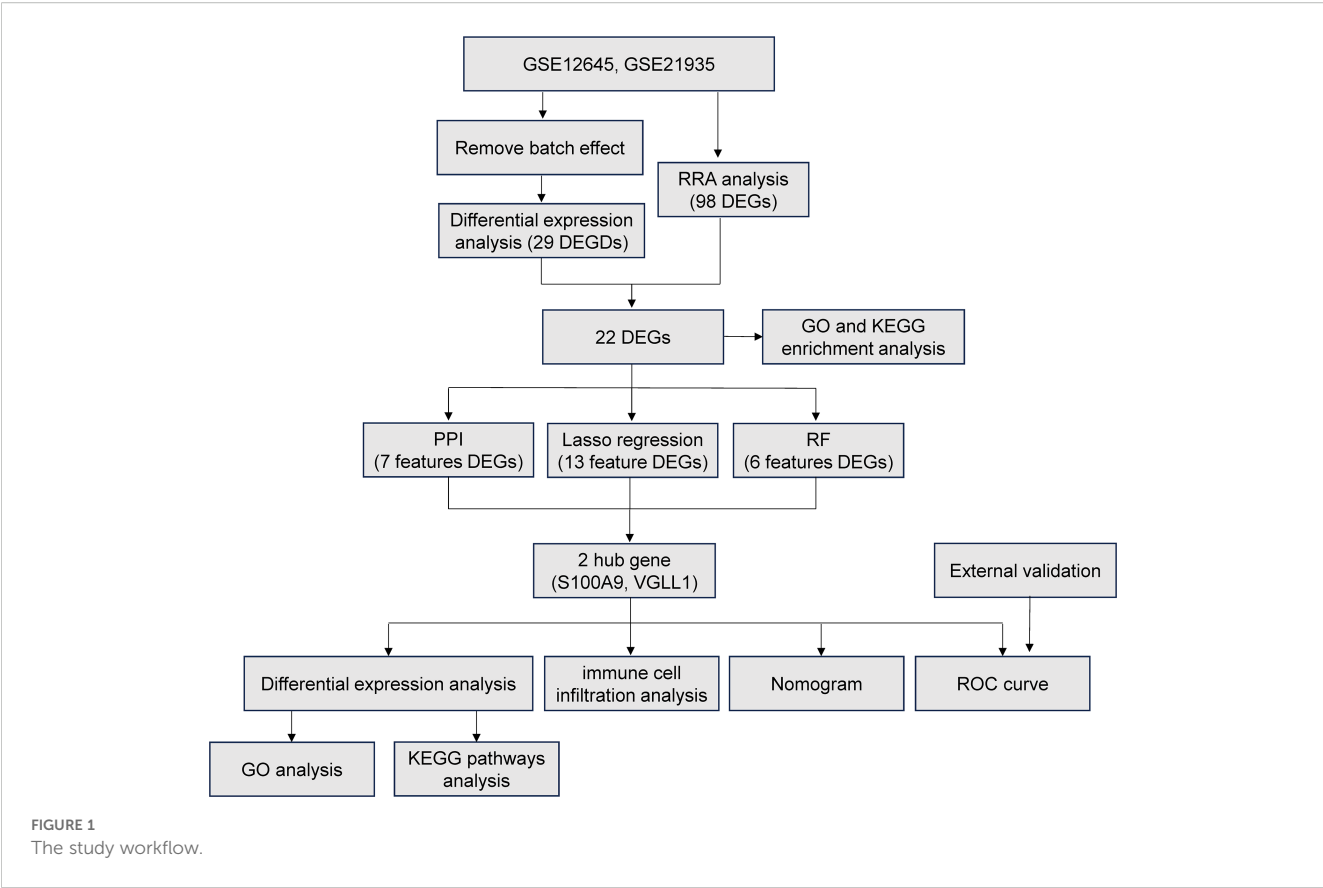
The study workflow was illustrated in Figure 1. After batch effect correction, showed significant improvements in sample clustering (Figures 2A–D). In the training cohort, a total of 29 DEGs were identified, including 16 downregulated and 13 upregulated genes (Figure 2E, Supplementary Table S1). Before RRA analysis, differential expression analyses were conducted separately on the GSE12654 and GSE21935 datasets, and the results were shown by volcano plots (Figures 3A, B). After integration using the RRA algorithm, a total of 98 DEGs were identified, comprising 41 downregulated and 57 upregulated genes (Figure 3C, Supplementary Table S2). Taking the intersection of these DEGs, we ultimately identified 22 significant DEGs (Figure 3D).

## 3.2 Enrichment analysis of DEGs

Subsequently, GO and KEGG enrichment analyses were performed on the 22 significant DEGs. The biological processes (BP) with high significance were related to nervous system development and function, including glial cell differentiation, astrocyte differentiation; Cellular component (CC) showed significant enrichment of DEGs in secretory granule lumen, collagen-containing extracellular matrix; Molecular function (MF) revealed significant enrichment of DEGs in carboxylic acid binding and organic acid binding (Figure 4A). KEGG pathway analysis further indicated that DEGs were enriched in several key signaling pathways involved in biological processes, such as IL-17, TNF and Hippo signaling pathways (Figure 4B).

## 3.3 Identification of hub genes

To systematically identify hub genes associated with disease pathogenesis, we first constructed PPI network to visualize the interactions among 22 DEGs. The results showed that 11 of the 22 DEGs had interactions (Figure 5A). Using 10 topological network



algorithms to rank genes, the intersection of the top 10 genes from each algorithm was taken, with a total of 7 genes (S100A9, CHI3L1, WWTR1, VGLL1, SERPINA3, S100A8, PVALB) identified as feature DEGs (Figure 5B). Subsequently, lasso regression and RF were employed to identify feature DEGs. Lasso regression analysis

selected 13 feature DEGs (MAG, VGLL1, S100A8, SPRR1A, ZNF345, S100A9, USH1C, NMU, SH2D2A, GPR45, SERPINA3, ARHGEF5, IGFBP2) (Figures 5C, D). while RF identified six feature DEGs (SH2D2A, WWTR1, MAG, VGLL1, KLK6, and S100A9) with Gini coefficients >2 (Figures 5E, F). Ultimately, through the



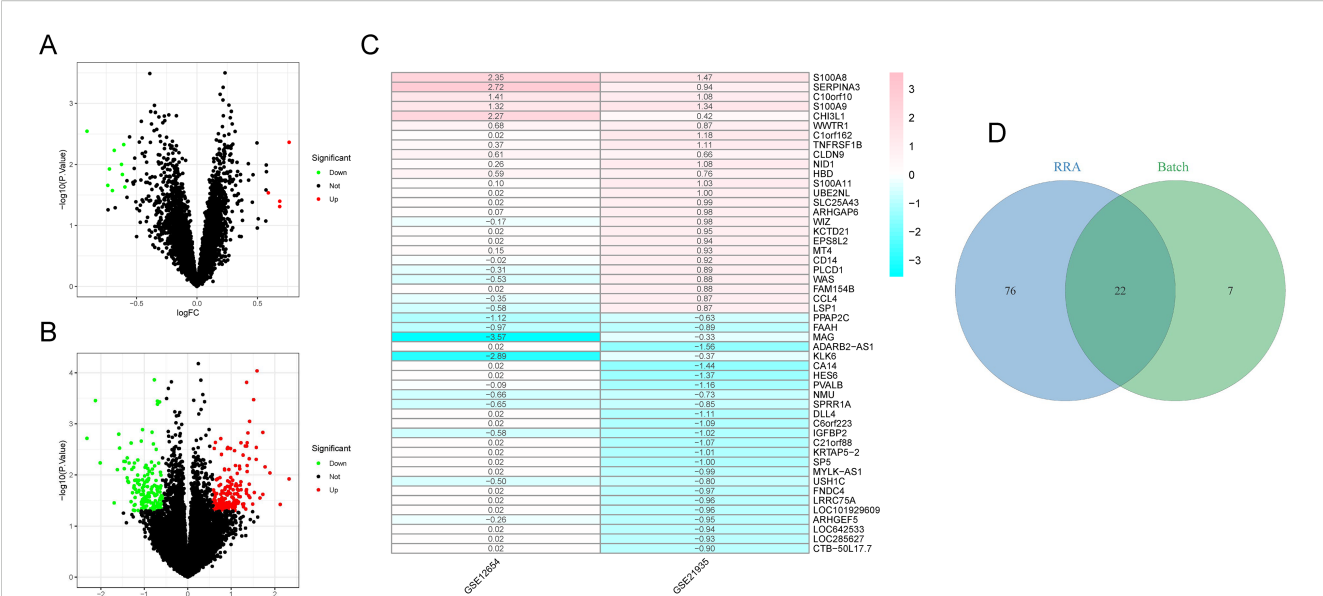


**FIGURE 3**  
RRA analysis. (A, B) Volcano plots of DEGs in GSE12654 and GSE21935 dataset. Red and green dots represent upregulated and downregulated DEGs, respectively. (C) Heatmap of 50 DEGs (25 upregulated and 25 downregulated) identified through RRA analysis. (D) Venn diagram showing the intersection of DEGs from the training cohort and RRA analysis.

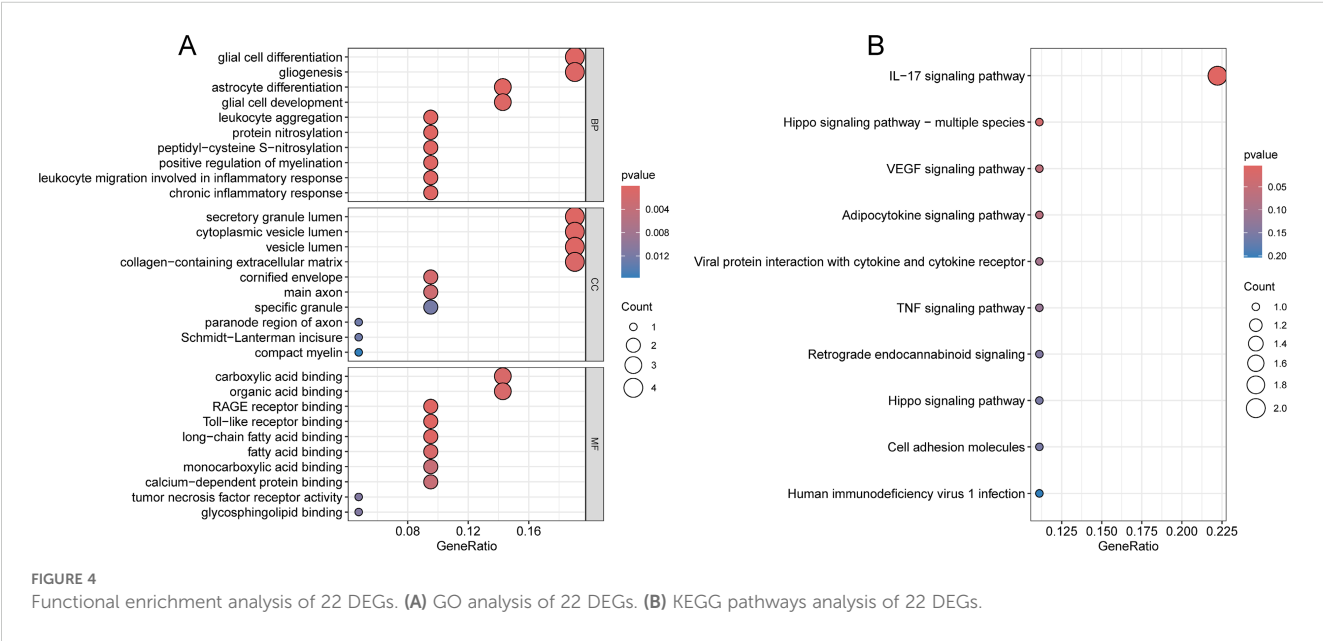


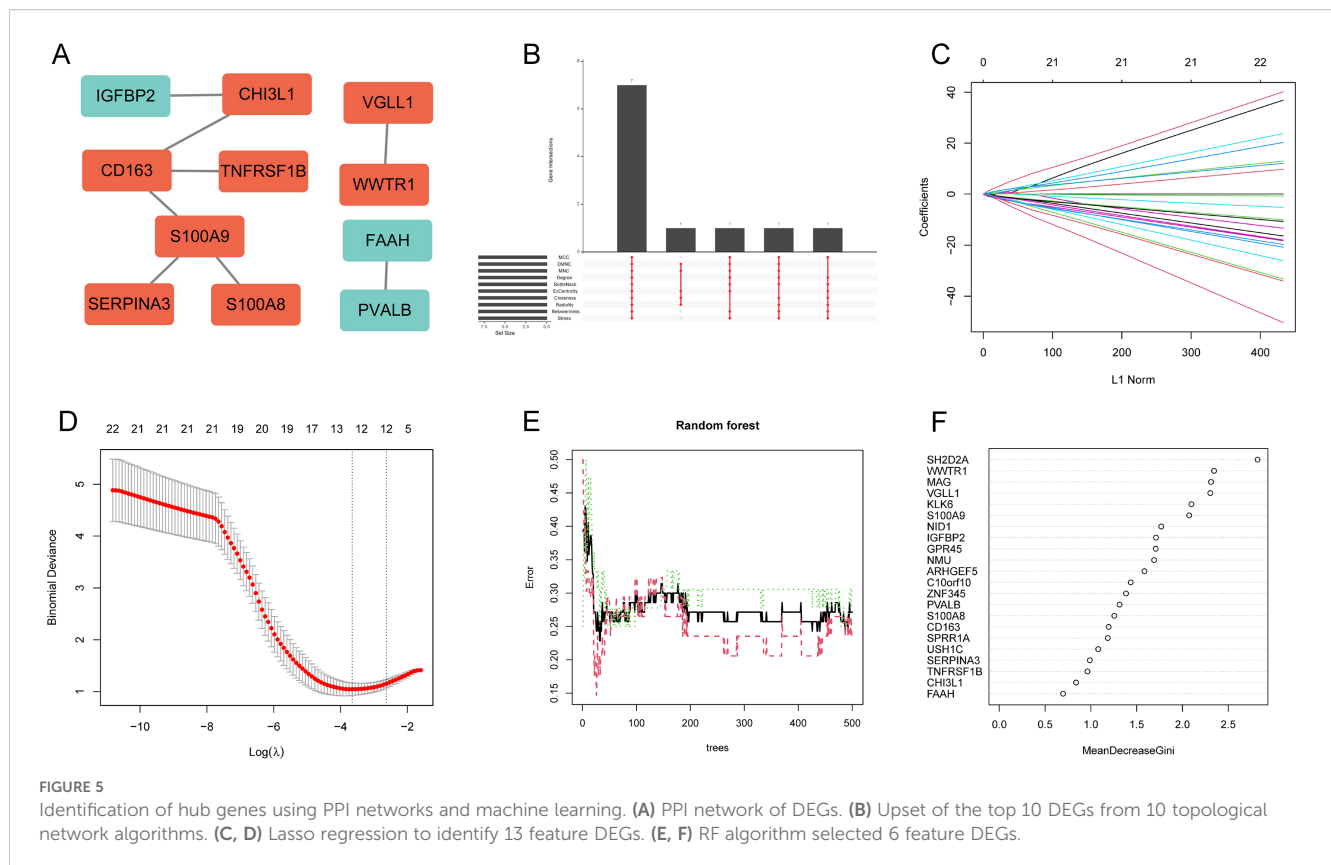
**FIGURE 4**  
Functional enrichment analysis of 22 DEGs. (A) GO analysis of 22 DEGs. (B) KEGG pathways analysis of 22 DEGs.

intersection analysis of these features DEG subsets, two DEGs (S100A9 and VGLL1) were determined as the optimal hub genes for SCZ (Figure 6A).

### 3.4 Construction and validation of the diagnostic model

The diagnostic value of the hub genes in SCZ was further evaluated. In the training cohort, S100A9 and VGLL1 were

significantly upregulated in SCZ groups (Figure 6B). The area under curve (AUC) values of ROC curve for these genes was 0.702 and 0.694, respectively (Figure 6C), indicating their diagnostic potential. Subsequently, a logistic diagnostic model was constructed based on the expression levels of S100A9 and VGLL1, with the formula:  $y = -1.4815 + 1.2469 \times VGLL1 + 0.4252 \times S100A9$ . The model achieved an AUC of 0.806 in the training cohort, demonstrating good discriminatory ability for SCZ (Figure 6D). Subsequently, we performed external validation of the predictive model's discriminative performance using gene expression profiles



of independent validation cohorts (GSE17612, GSE53987, and GSE38481). The results demonstrated that the model achieved AUC values of 0.702, 0.666, and 0.739 in the three external cohorts, respectively, further confirming its diagnostic efficacy and generalizability across independent datasets (Figures 6E–G). Additionally, we constructed a nomogram to predict the risk of SCZ (Figure 7A), and calibration curve analysis showed high consistency between predicted and actual SCZ risks (Figure 7B).

### 3.5 S100A9-related DEGs and functional enrichment analysis

To elucidate the potential molecular mechanisms of hub genes in the development of SCZ, we divided the SCZ samples in the training cohort into high- and low-expression groups based on the median expression of the hub genes and performed differential expression and functional enrichment analyses. Based on the median expression of S100A9, a total of 211 DEGs were identified, including 67 downregulated and 144 upregulated genes (Figure 8A, Supplementary Table S3). GO analysis (Figure 8B) indicated that S100A9-related DEGs were primarily involved in BP related to immune system regulation, such as regulation of immune effector process, leukocyte cell–cell adhesion, and cell activation involved in immune response. In terms of CC, DEGs were significantly enriched in external side of the plasma membrane and collagen-containing extracellular matrix. Regarding MF, DEGs were significantly enriched in cytokine binding, immune receptor

activity, and cell adhesion mediator activity. Additionally, KEGG pathway analysis showed that DEGs were primarily involved in the PI3K-Akt, HIF-1, and TNF signaling pathways (Figure 8C).

### 3.6 VGLL1-related DEGs and functional enrichment analysis

Based on the median expression of VGLL1, a total of 54 DEGs were identified, including 30 downregulated and 24 upregulated genes (Figure 8D, Supplementary Table S4). GO analysis showed that the main BP enriched by DEGs were also related to the immune system, such as leukocyte cell–cell adhesion and leukocyte adhesion to vascular endothelial cells; in addition, collagen-containing extracellular matrix, transport vesicles, growth factor activity, and heparin binding were significantly enriched in CC and MF (Figure 8E). KEGG pathway analysis further revealed that DEGs were significantly enriched in PI3K-Akt, TNF and IL-17 signaling pathways (Figure 8F). These results, similar to those of S100A9-related DEGs, suggest the important regulatory roles of the immune system and signaling pathways in the pathogenesis of SCZ.

### 3.7 Immune infiltration analysis

Given the enrichment analysis results indicating the involvement of hub genes in immune system responses, we further employed ssGSEA to analyze the infiltration levels of 28

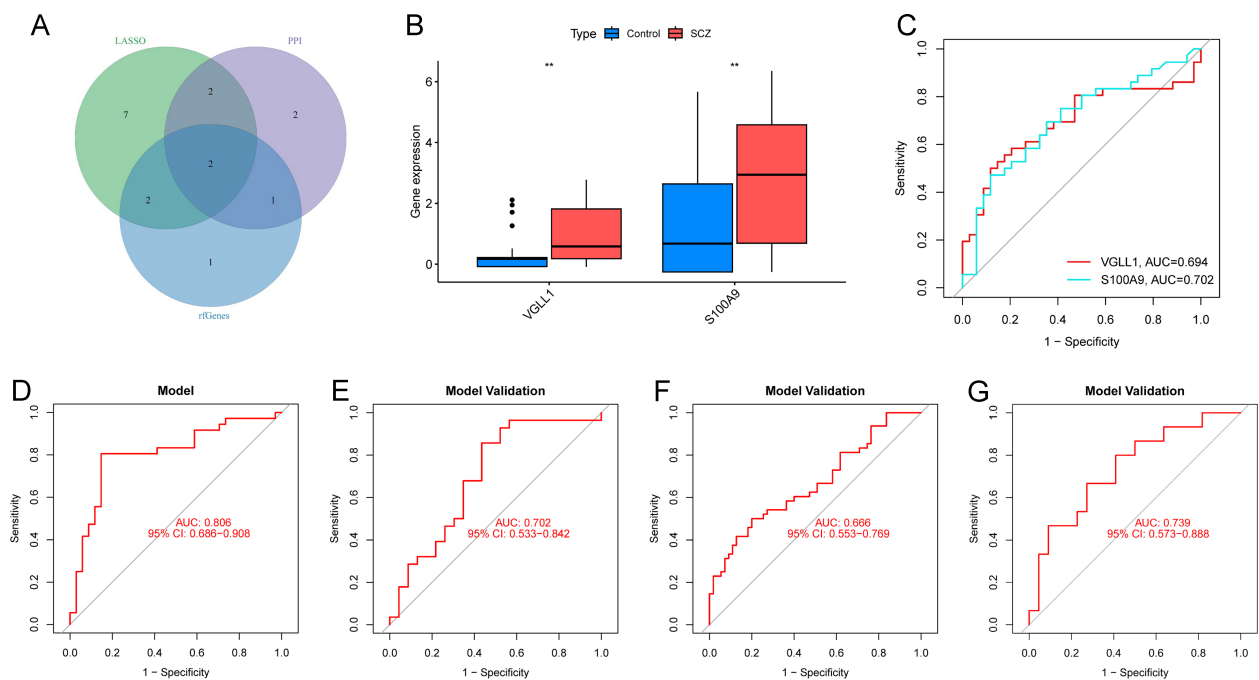


FIGURE 6

Identification and validation of the diagnostic model. (A) Intersection of feature DEGs from PPI network, lasso regression and RF algorithm. (B) Boxplots showing the differential expression of S100A9 and VGLL1 in training cohort. \*\* p-value < 0.01. (C) ROC curves for individual genes in training cohort. (D) ROC curve for diagnostic model in training cohort. (E–G) External validation in GSE17612 (E), GSE53987 (F) and GSE38481 (G).

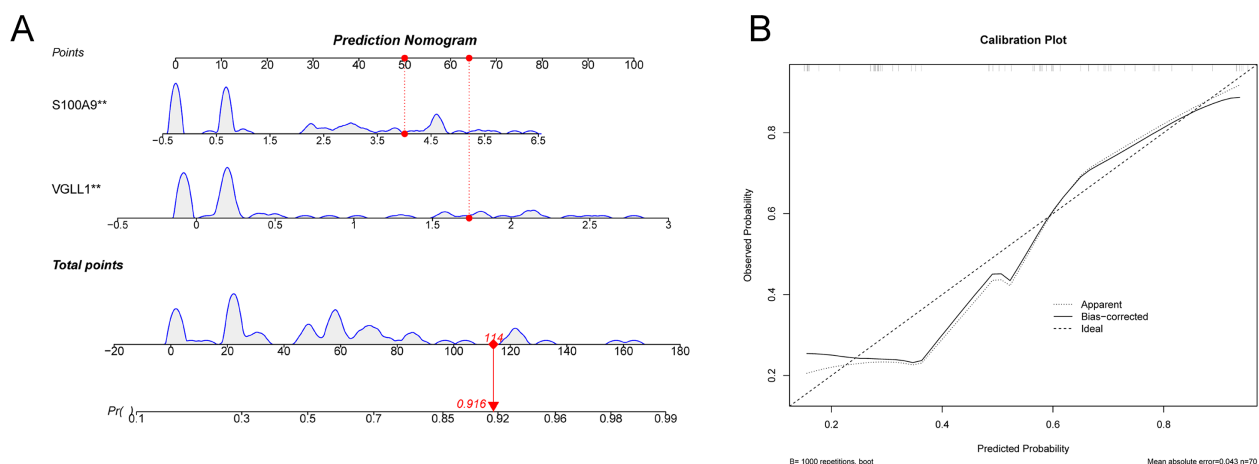


FIGURE 7

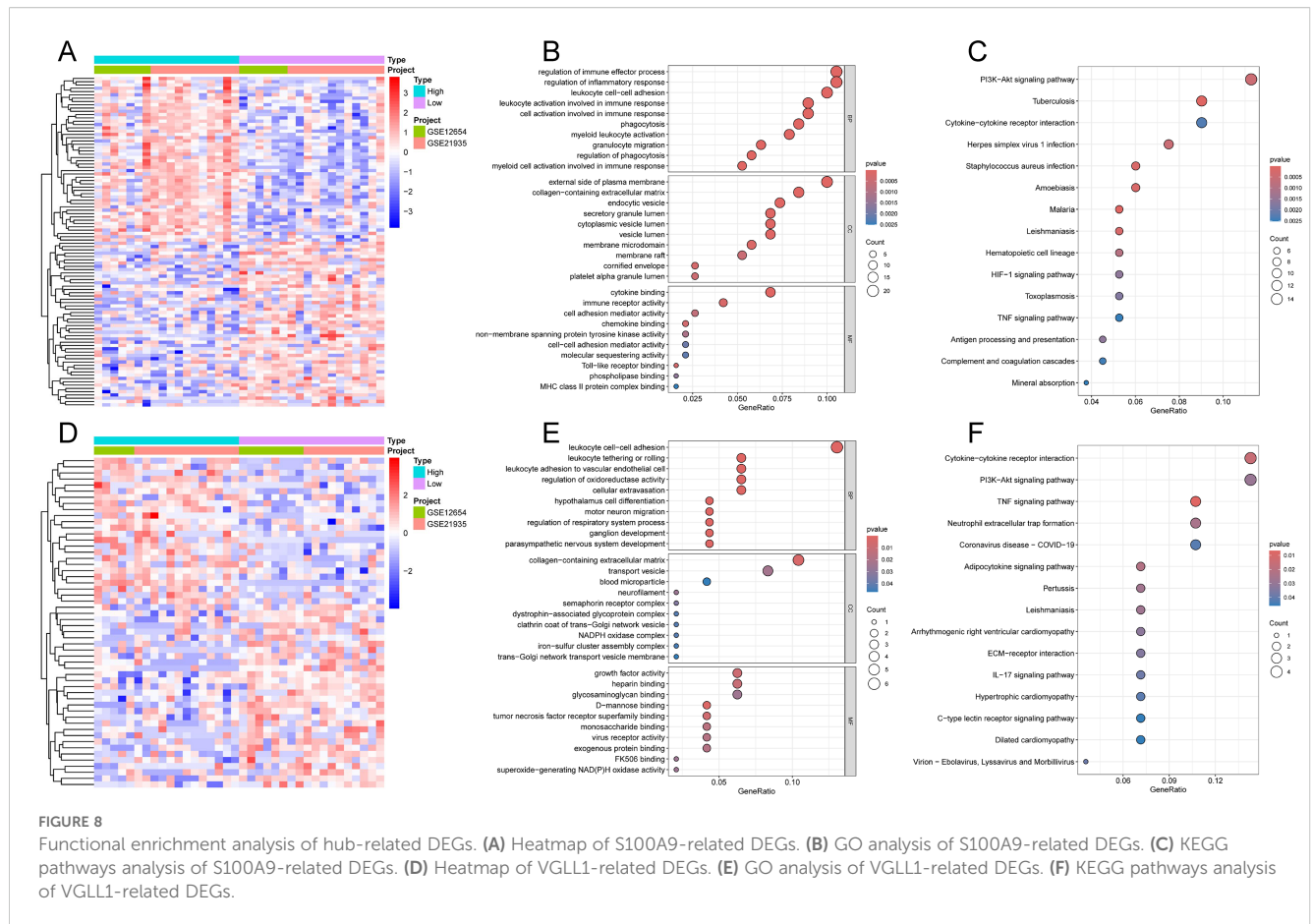
Nomogram and calibration curves for the diagnostic model. (A) The nomogram was used to predict the incidence of SCZ. (B) The calibration curve for evaluated the predictive power of the model.

immune cell types in the training cohort. The analysis revealed significant increases in the infiltration levels of five immune cell types in the SCZ group, including CD56bright natural killer cells, MDSCs, mast cells, natural killer cells, and plasmacytoid dendritic cells (Figure 9A). Correlation analysis further showed that S100A9 was significantly positively correlated with these immune cells, while VGLL1 was negatively correlated with plasmacytoid dendritic cells (Figures 9B, C). Collectively, our results suggest

that hub genes may be involved in the pathogenesis of SCZ through the regulation of immune cell infiltration.

## 4 Discussion

SCZ, a complex neuropsychiatric disorder with an incompletely elucidated etiology, arises from intricate interactions between



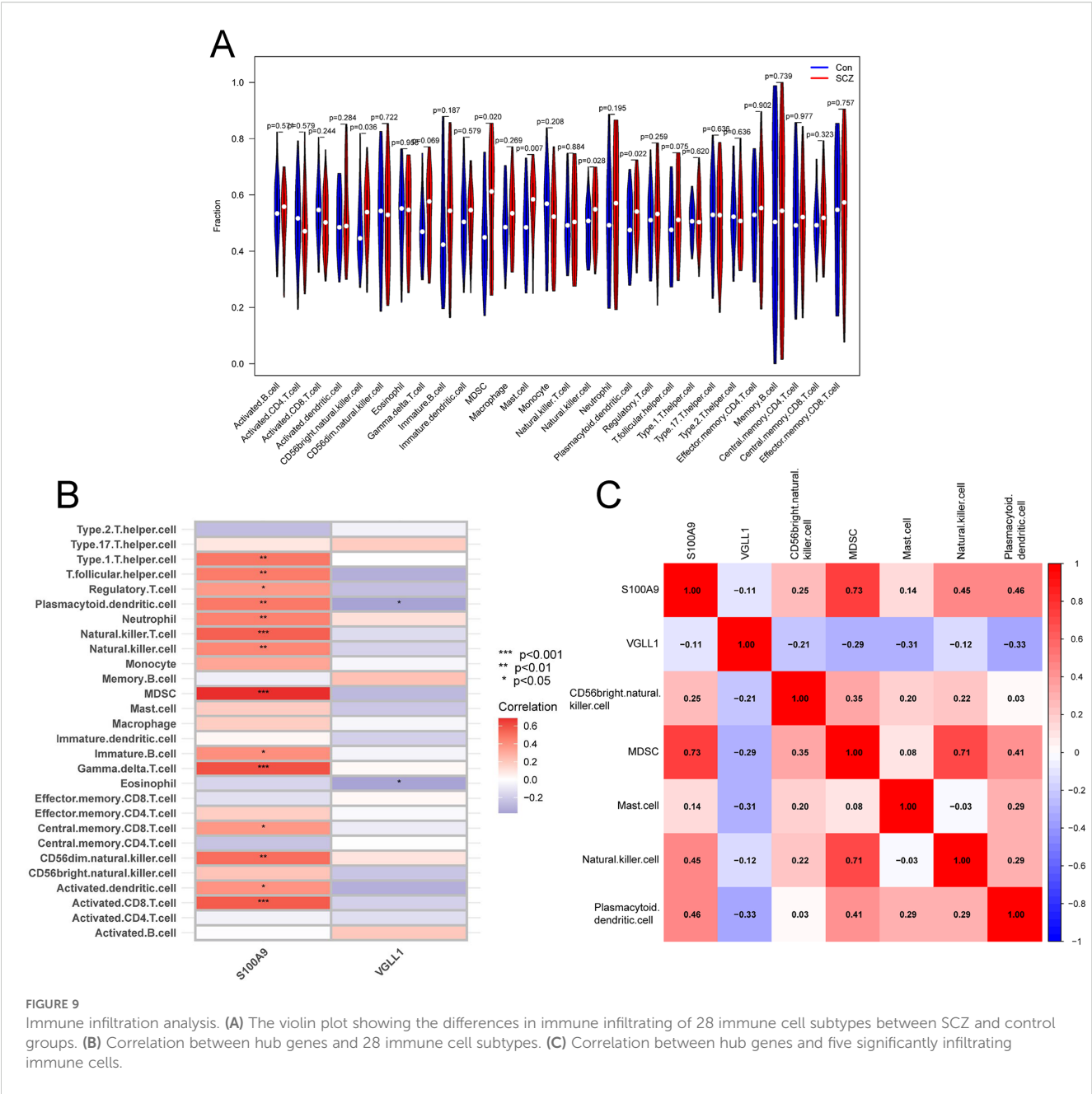
genetic predispositions and environmental factors (18). Emerging evidence highlights its association with dysregulated gene expression and immune system dysfunction (19). Although numerous studies have identified multiple genetic loci linked to SCZ, the critical genes driving its pathogenesis remain to be fully characterized (20). Given the substantial burden imposed by SCZ, the identification of novel diagnostic targets, coupled with exploration of the diversity and complexity of the immune microenvironment, is pivotal for achieving early diagnosis.

In this study, we employed integrated bioinformatics and machine learning to systematically screen SCZ-related biomarkers across multiple dimensions. Initially, differential expression analysis combined with RRA algorithm identified 22 significant DEGs. Subsequently the hub genes were further cross-identified through the PPI network and the RF and LASSO regression. Ultimately, we determined VGLL1 and S100A9 as potential diagnostic biomarkers for SCZ. A logistic regression model based on hub genes demonstrated good diagnostic performance in both the training cohort (AUC = 0.806) and external validation cohorts (AUC = 0.702 and 0.666), highlighting their clinical potential as SCZ biomarkers. Additionally, a nomogram based on the hub genes further demonstrated their potential for clinical application.

Subsequently, we explored the potential mechanisms of the hub genes in SCZ pathogenesis. Enrichment analysis revealed that S100A9- and VGLL1-related DEGs were primarily involved in

immune system regulation and key signaling pathways, including the PI3K-Akt and TNF signaling pathway. ssGSEA showed significant increases in the infiltration levels of five immune cell types in SCZ patients, including CD56bright natural killer cells, MDSCs, mast cells, natural killer cells, and plasmacytoid dendritic cells. Notably, S100A9 exhibited strong positive correlations with the infiltration of these immune cells, while VGLL1 showed a negative correlation with plasmacytoid dendritic cells.

The S100 protein family, implicated in neuroinflammation and astrocyte activation, is recognized as a contributor to schizophrenia pathogenesis. S100 proteins are significantly upregulated in the brain tissue, blood, and other body fluids of SCZ patients (21). S100A9, a pro-inflammatory calcium-binding protein within this family, is involved in various intracellular and extracellular biological processes, including cell differentiation, inflammatory responses, immune regulation, and intercellular signaling (22, 23). Recent studies have highlighted the role of S100A9 in the nervous system, particularly in neuropsychiatric disorders (24, 25). A recent study revealed that S100A9 drove microglial hyperactivation via the TLR4/NF- $\kappa$ B pathway, correlating with elevated neuroinflammatory markers in the cerebrospinal fluid of SCZ patients (26, 27). As a marker for MDSCs, S100A9 modulated MDSC-mediated immune suppression by binding to TLR4 and RAGE (28, 29). CD56bright natural killer cells, a subset of natural killer cells primarily secreting cytokines -IFN- $\gamma$ , exhibit increased percentages in acutely relapsed



SCZ patients, potentially serving as a disease trait marker (30, 31). Additionally, research found that S100A9 enhanced IFN- $\gamma$  production in NK cells via p38 MAPK pathway activation (32). Plasmacytoid dendritic cells are an important part of the immune system and are responsible for antigen presentation and cytokine secretion. Studies have shown that S100A9 was expressed on the surface of plasmacytoid dendritic cells, and when activated, S100A9 will be actively transported to the outside of the membrane, indicating that it may have biological functions (33). However, its exact role in plasmacytoid dendritic cells remains to be further confirmed. In summary, S100A9 may play an important role in immune regulation of schizophrenia through its interaction with multiple immune cells.

VGLL1, a transcriptional coactivator, regulates cell proliferation and differentiation by interacting with TEAD4, a transcription factor in the Hippo signaling pathway (34). Although its direct role in immune cells remains unclear, KEGG analysis indicated VGLL1-related DEGs were enriched in the PI3K-Akt signaling pathway, which is a crucial pathway for the activation and proliferation of various immune cells (35, 36). Thus, VGLL1 may modulate immune cell functions by influencing the PI3K-Akt signaling pathway. MDSCs suppress the functions of NK cells and T cells by secreting TGF- $\beta$  and IL-10 (37), and VGLL1 may indirectly affect the immunosuppressive functions of MDSCs by regulating these cytokine interactions. While no studies have explicitly linked VGLL1 to SCZ mechanisms, our findings provide initial insights into this point. Future research should investigate the



interactions between VGLL1 and immune regulation, as well as its role in the pathogenesis of SCZ, to determine whether it can serve as a potential target for diagnosis and treatment.

This study identified VGLL1 and S100A9 as novel diagnostic biomarkers for SCZ through integrated bioinformatics and machine learning, revealing their potential roles in disease progression through immune regulation. However, there are still some limitations. Firstly, potential limitations exist in the bioinformatics analytical methodology. For instance, data preprocessing approaches may introduce bias, as data selection and normalization procedures could lead to divergent analytical outcomes. Furthermore, the selected analytical tools (e.g., limma for differential expression analysis) have inherent limitations in their ability to fully capture the complexity of biological systems due to their predefined algorithms and assumptions. Second, all samples were derived from different public datasets, which may introduce heterogeneity in disease subtypes and clinical characteristics. This necessitates validation through independent clinical cohorts to ensure the robustness and generalizability of our findings. Thirdly, functional experiments are needed to elucidate the causal roles of the hub genes in SCZ. Finally, in future research, we could leverage single-cell sequencing to dissect the molecular interactions between specific brain regions and immune subpopulations, offering new directions for precision treatment of SCZ.

## Data availability statement

The original contributions presented in the study are included in the article/Supplementary Material. Further inquiries can be directed to the corresponding author.

## Author contributions

JL: Data curation, Formal Analysis, Writing – original draft. XW: Writing – review & editing. WQ: Conceptualization, Supervision, Writing – review & editing.

## Funding

The author(s) declare that no financial support was received for the research, and/or publication of this article.

## References

1. Carpenter WT, Tandon R. Psychotic disorders in DSM-5: summary of changes. *Asian J Psychiatr.* (2013) 6:266–8. doi: 10.1016/j.ajp.2013.04.001
2. GMD C. Global, regional, and national burden of 12 mental disorders in 204 countries and territories, 1990–2019: a systematic analysis for the Global Burden of Disease Study 2019. *Lancet Psychiatry.* (2022) 9:137–50. doi: 10.1016/s2215-0366(21)00395-3
3. Orrico-Sánchez A, López-Lacort M, Muñoz-Quiles C, Sanfélix-Gimeno G, Díez-Domingo J. Epidemiology of schizophrenia and its management over 8-years period using real-world data in Spain. *BMC Psychiatry.* (2020) 20:149. doi: 10.1186/s12888-020-02538-8
4. Furiak NM, Ascher-Svanum H, Klein RW, Smolen LJ, Lawson AH, Montgomery W, et al. Cost-effectiveness of olanzapine long-acting injection in the treatment of patients with schizophrenia in the United States: a micro-simulation economic decision model. *Curr Med Res Opin.* (2011) 27:713–30. doi: 10.1185/03007995.2011.554533
5. Du S, Liu J, Zhang Y, Ge X, Gao S, Song J. PD-L1 peptides in cancer immunoimaging and immunotherapy. *J Control Release.* (2025) 378:1061–79. doi: 10.1016/j.jconrel.2024.12.069
6. van Harten AC, Visser PJ, Pijnenburg YA, Teunissen CE, Blankenstein MA, Scheltens P, et al. Cerebrospinal fluid Aβ42 is the best predictor of clinical progression

## Conflict of interest

The authors declare that the research was conducted in the absence of any commercial or financial relationships that could be construed as a potential conflict of interest.

## Generative AI statement

The author(s) declare that no Generative AI was used in the creation of this manuscript.

Any alternative text (alt text) provided alongside figures in this article has been generated by Frontiers with the support of artificial intelligence and reasonable efforts have been made to ensure accuracy, including review by the authors wherever possible. If you identify any issues, please contact us.

## Publisher's note

All claims expressed in this article are solely those of the authors and do not necessarily represent those of their affiliated organizations, or those of the publisher, the editors and the reviewers. Any product that may be evaluated in this article, or claim that may be made by its manufacturer, is not guaranteed or endorsed by the publisher.

## Supplementary material

The Supplementary Material for this article can be found online at: <https://www.frontiersin.org/articles/10.3389/fpsy.2025.1621219/full#supplementary-material>

**SUPPLEMENTARY TABLE 1**  
29 DEGs of the training cohort.

**SUPPLEMENTARY TABLE 2**  
98 DEGs of RRA analysis.

**SUPPLEMENTARY TABLE 3**  
211 S100A9-related DEGs.

**SUPPLEMENTARY TABLE 4**  
54 VGLL1-related DEGs.

- in patients with subjective complaints. *Alzheimers Dement.* (2013) 9:481–7. doi: 10.1016/j.jalz.2012.08.004
7. Lee EE, Hong S, Martin AS, Eyler LT, Jeste DV. Inflammation in schizophrenia: cytokine levels and their relationships to demographic and clinical variables. *Am J Geriatr Psychiatry.* (2017) 25:50–61. doi: 10.1016/j.jagp.2016.09.009
8. Wang K, Li X, Wang X, Hommel B, Xia X, Qiu J, et al. *In vivo* analyses reveal hippocampal subfield volume reductions in adolescents with schizophrenia, but not with major depressive disorder. *J Psychiatr Res.* (2023) 165:56–63. doi: 10.1016/j.jpsychires.2023.07.012
9. Scott J, Crouse JJ, Medland SE, Mitchell BL, Gillespie NA, Martin NG, et al. Polygenic risk scores and help-seeking behaviour in young people with recent onset of mood and psychotic disorders. *J Affect Disord.* (2025) 372:40–7. doi: 10.1016/j.jad.2024.11.067
10. Bzdok D, Meyer-Lindenberg A. Machine learning for precision psychiatry: opportunities and challenges. *Biol Psychiatry Cognit Neurosci Neuroimaging.* (2018) 3:223–30. doi: 10.1016/j.bpsc.2017.11.007
11. Wu S, Jiang Q, Wang J, Wu D, Ren Y. Immune-related gene characterization and biological mechanisms in major depressive disorder revealed based on transcriptomics and network pharmacology. *Front Psychiatry.* (2024) 15:1485957. doi: 10.3389/fpsyt.2024.1485957
12. Feczko E, Balba NM, Miranda-Dominguez O, Cordova M, Karalunas SL, Irwin L, et al. Subtyping cognitive profiles in Autism Spectrum Disorder using a Functional Random Forest algorithm. *Neuroimage.* (2018) 172:674–88. doi: 10.1016/j.neuroimage.2017.12.044
13. Ni T, Sun Y, Li Z, Tan T, Han W, Li M, et al. Integrated transcriptome analysis reveals novel molecular signatures for schizophrenia characterization. *Adv Sci (Weinh).* (2025) 12:e2407628. doi: 10.1002/adv.202407628
14. Xie H, Wang J, Zhao Q. Identification of potential metabolic biomarkers and immune cell infiltration for metabolic associated steatohepatitis by bioinformatics analysis and machine learning. *Sci Rep.* (2025) 15:16596. doi: 10.1038/s41598-025-86397-x
15. Wenhui L, Nan W, Jiayi H, Ye X, Chunyu H, Zhongzhou L, et al. Prognostic analysis and identification of M7G immune-related genes in lung squamous cell carcinoma. *Front Immunol.* (2025) 16:1515838. doi: 10.3389/fimmu.2025.1515838
16. Subramanian A, Tamayo P, Mootha VK, Mukherjee S, Ebert BL, Gillette MA, et al. Gene set enrichment analysis: a knowledge-based approach for interpreting genome-wide expression profile. *Proc Natl Acad Sci U.S.A.* (2005) 102:15545–50. doi: 10.1073/pnas.0506580102
17. Barbie DA, Tamayo P, Boehm JS, Kim SY, Moody SE, Dunn IF, et al. Systematic RNA interference reveals that oncogenic KRAS-driven cancers require TBK1. *Nature.* (2009) 462:108–12. doi: 10.1038/nature08460
18. van Os J, Kapur S. Schizophrenia. *Lancet.* (2009) 374:635–45. doi: 10.1016/S0140-6736(09)60995-8
19. Mistry M, Gillis J, Pavlidis P. Genome-wide expression profiling of schizophrenia using a large combined cohort. *Mol Psychiatry.* (2013) 18:215–25. doi: 10.1038/mp.2011.172
20. Purcell SM, Wray NR, Stone JL, Visscher PM, O'Donovan MC, Sullivan PF, et al. Common polygenic variation contributes to risk of schizophrenia and bipolar disorder. *Nature.* (2009) 460:748–52. doi: 10.1038/nature08185
21. Shamir A, Yitzhaky A, Segev A, Haroutunian V, Katsel P, Hertzberg L. Up-regulation of S100 gene family in brain samples of a subgroup of individuals with schizophrenia: meta-analysis. *Neuromolecular Med.* (2023) 25:388–401. doi: 10.1007/s12017-023-08743-4
22. Chen Y, Ouyang Y, Li Z, Wang X, Ma J. S100A8 and S100A9 in cancer. *Biochim Biophys Acta Rev Cancer.* (2023) 1878:188891. doi: 10.1016/j.bbcan.2023.188891
23. Boucher J, Gilbert C, Bose S, Tessier PA. S100A9: the unusual suspect connecting viral infection and inflammation. *J Immunol.* (2024) 212:1523–9. doi: 10.4049/jimmunol.2300640
24. Sun Y, Wang Z, Hou J, Shi J, Tang Z, Wang C, et al. Shuangxinfang prevents S100A9-induced macrophage/microglial inflammation to improve cardiac function and depression-like behavior in rats after acute myocardial infarction. *Front Pharmacol.* (2022) 13:832590. doi: 10.3389/fphar.2022.832590
25. Sun Y, Wang Z, Wang C, Tang Z, Zhao H. Psycho-cardiology therapeutic effects of Shuangxinfang in rats with depression-behavior post acute myocardial infarction: Focus on protein S100A9 from proteomics. *BioMed Pharmacother.* (2021) 144:112303. doi: 10.1016/j.biopha.2021.112303
26. Qiao CM, Tan LL, Ma XY, Xia YM, Li T, Li MA, et al. Mechanism of S100A9-mediated astrocyte activation via TLR4/NF- $\kappa$ B in Parkinson's disease. *Int Immunopharmacol.* (2025) 146:113938. doi: 10.1016/j.intimp.2024.113938
27. Almeida PGC, Nani JV, Osés JP, Brietzke E, Hayashi MAF. Neuroinflammation and glial cell activation in mental disorders. *Brain Behav Immun Health.* (2020) 2:100034. doi: 10.1016/j.bbih.2019.100034
28. Özbay Kurt FG, Cicortas BA, Balzasch BM, De la Torre C, Ast V, Tavukcuoglu E, et al. S100A9 and HMGB1 orchestrate MDSC-mediated immunosuppression in melanoma through TLR4 signaling. *J Immunother Cancer.* (2024) 12:e009552. doi: 10.1136/jitc-2024-009552
29. Zhao F, Hoechst B, Duffy A, Gamrekashvili J, Fioravanti S, Manns MP, et al. S100A9 a new marker for monocytic human myeloid-derived suppressor cells. *Immunology.* (2012) 136:176–83. doi: 10.1111/j.1365-2567.2012.03566.x
30. Portales-Cervantes L, Dawod B, Marshall JS. Mast cells and natural killer cells-A potentially critical interaction. *Viruses.* (2019) 11:514. doi: 10.3390/v11060514
31. Miller BJ, Gassama B, Sebastian D, Buckley P, Mellor A. Meta-analysis of lymphocytes in schizophrenia: clinical status and antipsychotic effects. *Biol Psychiatry.* (2013) 73:993–9. doi: 10.1016/j.biopsych.2012.09.007
32. Li X, Hong L, Ru M, Cai R, Meng Y, Wang B, et al. S100A8/A9-activated IFN $\gamma$ (+) NK cells trigger  $\beta$ -cell necroptosis in hepatitis B virus-associated liver cirrhosis. *Cell Mol Life Sci.* (2024) 81:345. doi: 10.1007/s00018-024-05365-2
33. Lood C, Stenström M, Tydén H, Gullstrand B, Källberg E, Leanderson T, et al. Protein synthesis of the pro-inflammatory S100A8/A9 complex in plasmacytoid dendritic cells and cell surface S100A8/A9 on leukocyte subpopulations in systemic lupus erythematosus. *Arthritis Res Ther.* (2011) 13:R60. doi: 10.1186/ar3314
34. Yang Y, Jia W, Luo Z, Li Y, Liu H, Fu L, et al. VGLL1 cooperates with TEAD4 to control human trophectoderm lineage specification. *Nat Commun.* (2024) 15:583. doi: 10.1038/s41467-024-44780-8
35. Li Z, Zhang J, You S, Zhang J, Zhang Y, Akram Z, et al. Pterostilbene upregulates MICA/B via the PI3K/AKT signaling pathway to enhance the capability of natural killer cells to kill cervical cancer cells. *Exp Cell Res.* (2024) 435:113933. doi: 10.1016/j.yexcr.2024.113933
36. Nuiyen A, Sanguansermsri D, Sayasathid J, Thatsakorn K, Thapmongkol S, Ngoenkam J, et al. Nck1 regulates the *in vitro* development of human regulatory T cells through AKT pathway. *Clin Exp Immunol.* (2025) 219:uxaf011. doi: 10.1093/cei/uxaf011
37. Chen S, Zhu H, Jounaidi Y. Comprehensive snapshots of natural killer cells functions, signaling, molecular mechanisms and clinical utilization. *Signal Transduct Target Ther.* (2024) 9:302. doi: 10.1038/s41392-024-02005-w